

Flexural Strength of a Plain-Woven Tyranno-SA Fiber-Reinforced SiC Matrix Composite

Wen Yang¹, Hiroshi Araki¹, Akira Kohyama², Chumphol Busabok¹, Quanli Hu¹, Hiroshi Suzuki¹ and Tetsuji Noda¹

¹National Institute for Materials Science, Tsukuba 305-0047, Japan

²Institute of Advanced Energy, Kyoto University, Uji 611-0011, Japan

A SiC/SiC composite in a disc preform of 120 mm in diameter and 3.2 mm in thickness was fabricated by the chemical vapor infiltration (CVI) process. The composite was reinforced with plain-woven high-crystalline Tyranno-SA fiber. Microstructure examinations and density measurements indicated a quite dense and very good space homogeneous matrix deposition in the composite. The fracture behavior and statistic reliability of the flexural strength upon three-point bending loading were investigated. The composite had an average flexural strength 597 MPa with a standard deviation 70 MPa. The statistic analysis of the strength showed good consistency among the bending specimens, with a Weibull modulus of 10.2, which is much higher than that for the Nicalon and Hi-Nicalon fibers reinforced CVI-SiC matrix SiC/SiC composites.

(Received May 12, 2003; Accepted July 11, 2003)

Keywords: Tyranno-SA fiber, SiC/SiC composite, chemical vapor infiltration, flexural strength

1. Introduction

Ceramic materials possess excellent thermal properties, oxidation resistance and strength *etc.*, but the applications are markedly limited by the catastrophic failure behavior. However, the fracture tolerance of ceramic materials can be significantly improved by the incorporation of reinforcement fibers, particles or whiskers. During the past several tens of years, many efforts have been done to develop continuous silicon carbide fibers reinforced silicon carbide matrix (SiC/SiC) composites for use in energy conversion systems, aviation and aerospace systems, *etc.*¹⁻⁴⁾ SiC/SiC composites usually exhibit relatively large scatter in strength^{5,6)} because of the statistic distributions of the flaws and pores in the materials. Therefore, fabrication of SiC/SiC composites with dense and space homogeneous matrix densification is critical and remains one of the main current issues, especially when it comes to the evaluation of the strength and reliability of SiC/SiC composites, which is necessary for critical engineering applications.

The empirical Weibull distribution is widely used to evaluate the reliability of ceramic materials including particles or fibers/whiskers reinforced composites.⁷⁻⁹⁾ The Weibull distribution describes the probability of failure of the strength of a material (specimen), P , at a given stress, σ , as the function of its tested volume, V :

$$P(\sigma) = 1 - \exp \left[-\frac{V}{V_0} \times \left(\frac{\sigma - \sigma_u}{\sigma_0} \right)^m \right] \quad (1)$$

where V_0 and σ_0 are scaling constants. m is the Weibull-shape parameter (Weibull modulus), which characterizes the dispersion of the failure strength. The smaller the value of m the greater the strength dispersion. σ_u is the strength below which no failure occurs. For the highest reliability, σ_u can be set equal to zero,¹⁰⁾ resulting in the flexible two-parameter Weibull distribution as:

$$P(\sigma) = 1 - \exp \left[-\frac{V}{V_0} \times \left(\frac{\sigma}{\sigma_0} \right)^m \right] \quad (2)$$

Using the Weibull distribution, Quinn¹⁰⁾ made a detailed statistic study on the flexural strength data of sintered alumina and reaction-bonded silicon nitride ceramics from seven different laboratories. Wilson¹¹⁾ and Parthasarathy¹²⁾ studied the Weibull tensile strength distribution of NextelTM 610 and NextelTM 720 fibers and Nicalon fiber, respectively. The Weibull modulus of the reinforcement fibers in continuous fiber reinforced ceramic matrix composites (CFCC) generally have substantial effects on the ultimate strength and fiber pullout behaviors, as demonstrated by Curtin *et al.*¹³⁾ and others.^{9,14,15)} Dutton¹⁴⁾ predicted the ultimate tensile strength of a unidirectional glass-matrix composite with a model, Global Load-Sharing Model, developed by Curtin, which relates the ultimate tensile strength of CFCC to the Weibull modulus of the fiber, the fiber volume fraction, and a characteristic strength, σ_c .¹⁴⁾ The prediction was compared with the experimental results. Sutcu¹⁵⁾ applied the Weibull theory to estimate the fiber pullout in ceramic composites and the work of fracture. The effects of Weibull modulus of fiber on the failure behaviors in the composites were discussed, and good agreement was observed when the predicted stress-strain curve upon tension was compared with the experiment results on a LAS-Glass/Nicalon fiber composite. Ismar⁹⁾ carried out a computational effort to simulate the mechanical behavior of SiC/SiC composites upon tension load based on assumptions of the Weibull strength distributions of all the three key factors for CFCC, the fiber, the matrix, and the interface. The effects of the fiber volume fraction and Weibull modulus were discussed. However, the above mentioned studies relating to CFCC either studied the Weibull strength distribution of the reinforcement fiber itself, or predicted the mechanical properties of the composites based on the assumption of Weibull distributions of the constituents (the fiber, matrix and interphase) and compared the theoretical prediction with the experimental results. Furthermore, the above established understandings on SiC/SiC composites are for those reinforced with old-generation SiC fibers such as Nicalon or Hi-Nicalon. The SiC fiber technology is rapidly developing. Recently, a new SiC fiber,

Tyranno-SA, is successfully developed.¹⁶⁾ This fiber exhibits outstanding high temperature strength, coupled with much improved thermal conductivity and thermal stability compared with the Nicalon and Hi-Nicalon fibers. The fabrication cost of the Tyranno-SA fiber is also reduced to near half of that of the Hi-Nicalon fiber.¹⁷⁾ The Tyranno-SA fiber makes SiC/SiC composites even more attractive for the many applications.^{1–4,17)}

In this study, effort was first made to fabricate a plain-woven Tyranno-SA fiber reinforced SiC matrix composite using the chemical vapor infiltration (CVI) process with uniformly densified matrix. Flexural fracture behavior of the materials was studied, and the statistical analysis of the flexural strength was conducted using the Weibull theory.

2. Experimental

2.1 Composite fabrication

2D plain-woven Tyranno-SA fiber cloths laminated with 17 sheets were used as the composite preform. The preform was compressed with a set of graphite fixtures to keep a fiber volume fraction of $\sim 30\%$, resulting in a dimension of the preform 120 mm in diameter and 3.2 mm in thickness. The preform was then pre-coated with 250 nm thick pyrolytic carbon (PyC) as fiber-matrix interlayer from methane (CH_4) using the CVI process, to modify the interfacial shear/sliding strength. The pre-coated perform was finally densified with SiC-matrix using the thermal decompositions of methyletri-chlorosilane (MTS), having a purity higher than 99 vol%. MTS was carried by hydrogen with a reduced pressure of 14.4 kPa in the CVI reactor. A hydrogen by-path system was also used for a fine control of the volume ratio of the MTS to hydrogen, which was found¹⁸⁾ critical to the density and space uniformity of the final deposited matrix. The CVI densification process was carried out at 1323 K for 80 hours. The volume ratio of the MTS to hydrogen was kept at 0.5 with a total hydrogen flow rate 2.0 l/min. The CVI process conditions were designed based on a detailed investigation on the effects of the process conditions on the densification process.¹⁸⁾

Bars with a surface area of $25 \text{ mm} \times 4.0 \text{ mm}$ were cut parallel to one of the fiber bundle directions of the fabric cloth from half of the composite after the CVI process, as shown in Fig. 1, to investigate the matrix space homogeneity. Both surfaces of the specimens (bars) were carefully ground with diamond slurry ($9 \mu\text{m}$) to remove the surface CVD (chemical vapor deposition)-SiC layer that was formed at the end of the CVI. Another purpose of the careful surface grinding is to guarantee a same surface condition of the specimen for the following bending test. The resulting specimen size was 25 mm in length, 4.0 mm in width and 2.0 mm in thickness. The density of each bar was measured from its mass and volume before bending test. The space homogeneity of microstructure was inspected by means of scanning electron microscope (SEM).

2.2 Three-point bending tests

Three-point bending tests were carried out for the bars at room temperature with the load in the vertical direction to the laminates. The simple three-point bending test was used for

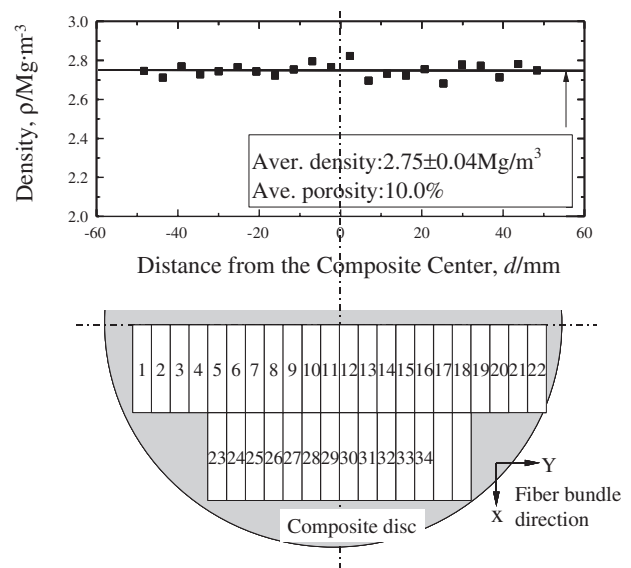


Fig. 1 Density and space homogeneity of the composite.

comparison with the literature reports on the Nicalon and Hi-Nicalon fibers reinforced SiC/SiC composites. Totally 34 specimens were tested. The cross-head speed was adjusted to 0.0083 mm/s. The ultimate flexural strength (σ) was obtained from the load-displacement curves using the simple beam theory:

$$\sigma = \frac{3}{2} \frac{FL}{WT^2} \quad (3)$$

where F is the flexural load. L is the load-supporting span that is 16 mm in this study. W and T are the width and thickness of the specimen, respectively. The microstructure and fracture surfaces were examined with SEM.

3. Results and Discussion

3.1 Matrix space homogeneity

Figure 1 illustrates the bending specimens densities with respect to their original positions in the composites (specimen from No. 1 to No. 22). The highest density among the 22 specimens is as high as 2.82 Mg/m^3 (corresponding to a porosity 9.5%), while the lowest, 2.67 Mg/m^3 . Figure 1 shows a quite narrow density distribution of the 22 specimens, and no clear space-dependence of the density/matrix densification was observed. The densities of all the 34 specimens are listed in Table 1. The average density is 2.75 Mg/m^3 with a standard deviation 0.04 Mg/m^3 , achieving a very small coefficient of variation (CV), 0.015.

Figure 2 shows the cross-section (Fig. 2(a)) and the intra-fiber bundles microstructure (Fig. 2(b)) of specimen No. 28. The density of the specimen is 2.75 Mg/m^3 , same as the average density. Some inter-fiber bundles pores with the length about $500 \mu\text{m}$ is evidenced in Fig. 2(a) while small pores ($20\text{--}30 \mu\text{m}$ or smaller) is found in the intra-fiber bundles area (Fig. 2(b)). However, although some inter-/intra-bundles pores still exist in the specimen, the specimen was densely deposited with matrix considering the high average density. SEM observations of other specimens revealed similar microstructures as shown in Fig. 2. Figures

Table 1 The density and flexural strength of the composite.

Specimen No.	Density, Mg/m ³	σ , MPa
1	2.74	674
2	2.70	475
3	2.76	661
4	2.72	686
5	2.73	513
6	2.76	600
7	2.73	549
8	2.71	681
9	2.74	535
10	2.79	483
11	2.76	525
12	2.82	629
13	2.69	583
14	2.72	677
15	2.71	721
16	2.75	568
17	2.67	568
18	2.79	588
19	2.76	674
20	2.70	573
21	2.77	610
22	2.74	571
23	2.73	596
24	2.68	496
25	2.73	642
26	2.77	514
27	2.74	659
28	2.75	635
29	2.76	642
30	2.81	565
31	2.83	651
32	2.74	608
33	2.75	454
34	2.81	687

1 and 2 indicate a quite dense matrix densification of current composite by the CVI process with very good space homogeneity.

3.2 Fracture behaviors and flexural strength

Figure 3 shows a typical load-displacement curve of the specimen. The curve demonstrates an initial linear behavior, followed by a relatively small nonlinear domain of deformation until the load maximum, due mainly to the matrix cracking, interfacial debonding and fiber sliding, and the failure of substantial fraction of fibers. The specimen still supports a load about 60 N after reached the maximum load to a displacement up to near 0.35 mm, indicating a small amount of the fibers survived the first main fracture of the specimen and enabled the material to bear some load till larger deformation. The fracture surface and fiber pullout of this specimen are shown in Fig. 4. Interfacial debonding and relatively short fiber pullout ($\sim 10\mu\text{m}$ or less) occurred during the failure of the specimen, as evidenced in Fig. 4(b).

The flexural strengths are listed in Table 1. The highest strength, 721 MPa, was achieved in specimen No. 15, and the

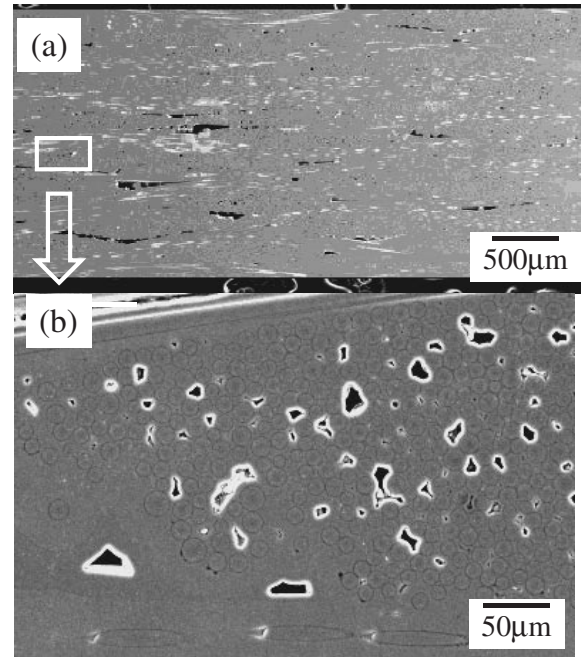


Fig. 2 SEM images of cross-section ((a)) and intra-fiber bundles micro-structure ((b)) of specimen No. 28.

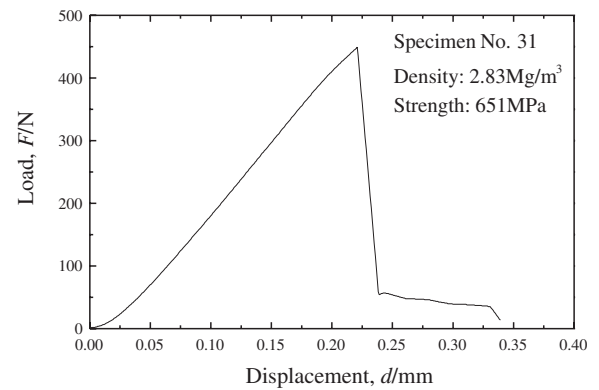


Fig. 3 Representative load-displacement curve.

Table 2 Statistic reliability of flexural strength of the composite.

Ave. strength MPa	Standard dev. MPa	CV	m	m_{CV}
597	70	0.117	10.2	10.3

lowest, 475 MPa, in No. 2. The composite had a quite high average strength, 597 MPa, with a relatively small standard deviation 70 MPa, as shown in Table 2. The coefficient of variation is 0.117.

3.3 Weibull statistic distribution of the strength

The strength is assumed to follow the Weibull distribution, and the strength σ_u is defined to be zero for the highest safety. By taking the natural logarithm of both sides of eq. (2), the following equation is obtained:

$$\ln[\ln(1/(1 - P))] - \ln(V/V_0) = m \ln(\sigma/\sigma_0) \quad (4)$$

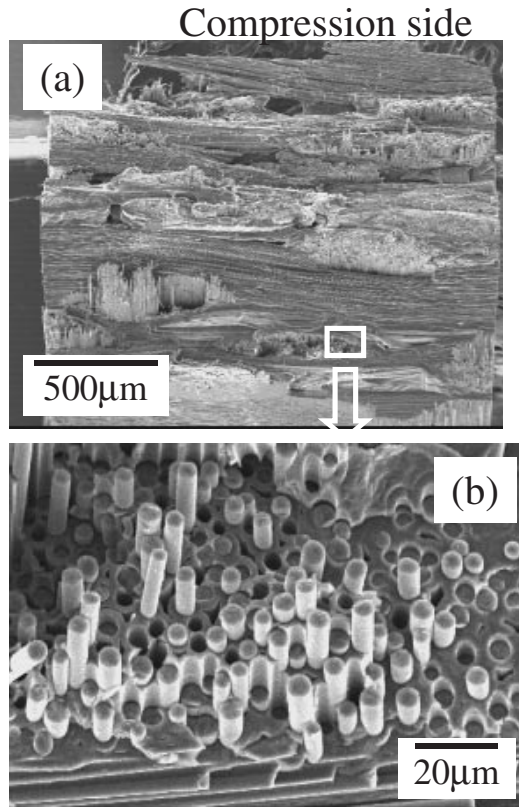


Fig. 4 SEM images of fracture surface and interfacial debonding/fiber pullout behaviors of specimen No. 31.

Since the bending tests were conducted with constant testing volume, eq. (4) is reduced to:

$$\ln[\ln(1/(1-P))] = m \ln \sigma + k \quad (5)$$

where k is a constant. The Weibull modulus of the flexural strength can be determined by plotting $\ln[\ln(1/(1-P))]$ against $\ln \sigma$.

The cumulative probability of failure is determined by:¹⁰⁾

$$P_i = \frac{i - 0.5}{N} \quad (6)$$

where P_i is the cumulative probability of failure of the i th specimen ranked from the lowest strength to the highest one. N is the total number of specimens, 34, in this study.

Figure 5 shows the cumulative probability of failure of normalized flexural strength. The strength of each specimen was normalized by the average strength. Figure 5 shows that approximately 60% of the specimens failed within 10% of the average strength, and all the data, except the lowest and the highest ones, fall into the 20% of the average strength. Figure 5 indicates a rather high degree of consistency among present specimens.

The Weibull plot is shown in Fig. 6. The calculated Weibull modulus is 10.2. The data was fitted using the least-square method. The two-parameter Weibull equation fits the data quite well although some deviation from the best-fit line occurred at the low strength extreme and slightly at the high strength extreme.

The Weibull modulus can also be estimated from the CV as:¹¹⁾

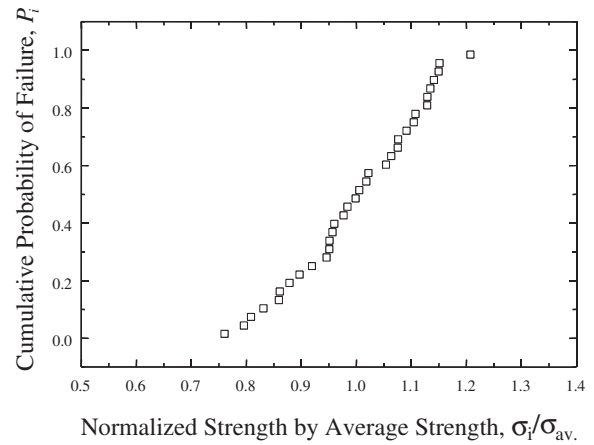


Fig. 5 Cumulative probability of failure of normalized flexural strength.

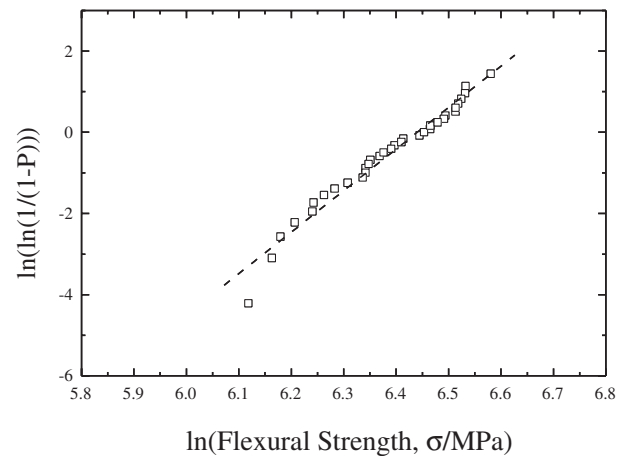


Fig. 6 Weibull plot for the flexural strength.

$$m_{CV} = 1.2/CV \quad (7)$$

This estimation is very accurate when the Weibull modulus is higher than 10. Using this method, the Weibull modulus of present flexural strength was calculated to be 10.3, which is in very good agreement with the result by the normal Weibull analysis, as shown in Table 2.

Araki *et al.*¹⁹⁾ has reported a recent statistic study on the flexural strengths of Nicalon and Hi-Nicalon fibers reinforced SiC/SiC composites. Their results are shown in Fig. 7. These composites were fabricated using the same CVI system and process conditions as in present study. Figure 7 shows a very low Weibull modulus, 2.1, for the Nicalon fiber reinforced composite. Improved Weibull modulus, 7.4, was obtained for the Hi-Nicalon fiber reinforced one but it is still much lower than that of the present Tyranno-SA/SiC composite.

The strength statistics of the Nicalon and Hi-Nicalon fibers have been studied by Eckel *et al.*²⁰⁾ and Bertrand *et al.*,²¹⁾ respectively, using the fracture mirror radius approach²⁰⁾ and tensile tests on single filaments.²¹⁾ The reported Weibull moduli (m_f) were 3.5 (average value of the reported data, 2.3–4.6, by Eckel *et al.*) and 4.2 for the Nicalon and Hi-Nicalon fibers, respectively. The Weibull modulus of the Nicalon fiber was slightly lower than that of the Hi-Nicalon fiber but the Nicalon/SiC composite showed much lower

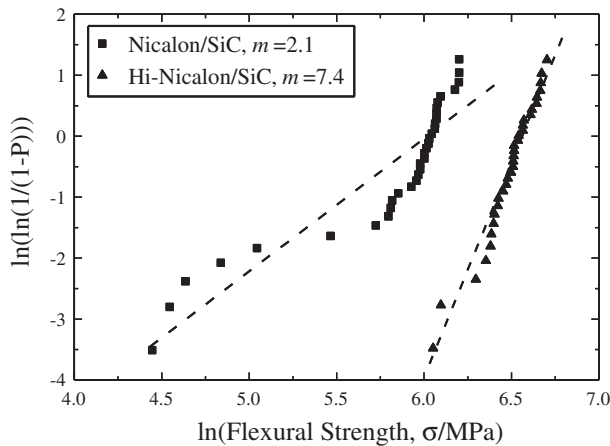


Fig. 7 Weibull plots for the flexural strengths of Nicalon and Hi-Nicalon fibers reinforced SiC/SiC composites by Araki *et al.*¹⁹⁾

flexural strength Weibull modulus than that of the Hi-Nicalon/SiC composite (Fig. 7). The much lower Weibull modulus of the Nicalon/SiC composite was mainly attributed to possible significant degradation of the fibers during the CVI process at 1323 K for 80 hours¹⁹⁾ due to its thermodynamically unstable at high temperatures. For the present Tyranno-SA fiber, the strength Weibull modulus was unavailable in the current literature. The widely used empirical fracture mirror radius approach for the Nicalon and Hi-Nicalon fibers is inapplicable either because no fracture mirror structure was found at the cross sections of fractured Tyranno-SA fibers in present study, as well as a previous study.²²⁾ However, here the strength Weibull modulus of the Tyranno-SA fiber was roughly estimated to be 7.6 using the reported strength data¹⁶⁾ via eq. (7), which is much higher than those of the Nicalon and Hi-Nicalon fibers, resulting in a similar trend of the strength Weibull moduli of their composite counterparts. The above analysis indicates that the strength statistics of the fibers has significant affections on the strength distributions of the SiC/SiC composites. The reinforcement fibers with large strength Weibull modulus result in small scattering of the strength of the composite, which can obtain even higher strength Weibull modulus than the reinforcement fibers likely due to the contributions from the matrix and/or the interface.

4. Conclusions

With appropriate process conditions, SiC/SiC composite reinforced with plain-woven Tyranno-SA fabrics in a disc preform 120 mm in diameter and 3.2 mm in thickness was fabricated by the CVI with quite dense and space homogeneous matrix densification. The statistic reliability of the strength upon three-point bending was studied. High degree of flexural strength consistency among the specimens was shown. The composite had an average flexural strength 597 MPa with a standard deviation 70 MPa. Interfacial

debonding and relatively short fiber pullout were observed with SEM examination of the fracture surfaces of the specimens. The Weibull distribution gave a good expression of the statistic reliability of the flexural strength for present Tyranno-SA/SiC composite. By fitting the data using the least-square method, the Weibull modulus of the flexural strength was calculated to be 10.2. This study indicates that the strength statistics of the fibers has significant affections on the strength distributions of the SiC/SiC composites. The reinforcement fibers with large strength Weibull modulus result in small scattering of the strength of the composite. Whereas the SiC/SiC composite can obtain a strength Weibull modulus higher than its reinforcement fibers likely due to the contributions from the matrix and/or the interface.

Acknowledgements

This work is supported by the CREST, Japan Science and Technology Corporation and conducted at the Institute of the Advanced Energy, Kyoto University. A part of this study was financially supported by the Budget for Nuclear Research of the Ministry of Education, Culture, Sports, Science and Technology, based on the screening and counseling by the Atomic Energy Commission.

REFERENCES

- 1) T. Hinoki, Y. Katoh and A. Kohyama: *Mater. Trans.* **43** (2002) 617–621.
- 2) A. G. Evans and D. B. Marshall: *Acta Metall.* **37** (1989) 2567–2583.
- 3) D. Brewer: *Mater. Sci. Eng.* **A261** (1999) 284–291.
- 4) P. Fenici and H. W. Scholz: *J. Nucl. Mater.* **212–215** (1994) 60–68.
- 5) W. Yang, H. Araki, T. Noda, J. Y. Park, Y. Katoh, T. Hinoki, J. Yu and A. Kohyama: *Mater. Trans.* **43** (2002) 2568–2573.
- 6) E. Lara-Curzio: *Properties of CVI-SiC Matrix Composites*, (Elsevier Comprehensive Composites Encyclopedia, 2000) pp. 533–577.
- 7) C. A. Folsom, F. W. Zok and F. F. Lange: *J. Am. Ceram. Soc.* **77** (1994) 689–696.
- 8) G. Quinn: *J. Am. Ceram. Soc.* **73** (1990) 2374–2384.
- 9) H. Ismar and F. Streicher: *Comp. Mater. Sci.* **16** (1999) 17–24.
- 10) B. Bergman: *J. Mater. Sci. Lett.* **3** (1984) 689–692.
- 11) D. M. Wilson: *J. Mater. Sci.* **32** (1997) 2535–2542.
- 12) T. A. Parthasarathy: *J. Am. Ceram. Soc.* **84** (2001) 588–592.
- 13) W. A. Curtin: *J. Am. Ceram. Soc.* **74** (1991) 2837–2845.
- 14) R. E. Dutton, N. J. Pagano, R. Y. Kim and T. A. Parthasarathy: *J. Am. Ceram. Soc.* **81** (2000) 166–174.
- 15) M. Sutcu: *Acta. Metall. Mater.* **37** (1989) 651–661.
- 16) T. Ishikawa, Y. Kohtoku, K. Kumagawa, T. Yamamura and T. Nagasawa: *Nature* **391** (1998) 773–775.
- 17) A. Kohyama, M. Seki, K. Abe, T. Muroga, H. Matsui, S. Jitsukawa and S. Matsuda: *J. Nucl. Mater.* **283–287** (2000) 20–27.
- 18) W. Yang: *Development of CVI Process and Property Evaluation of CVI-SiC/SiC Composites*, *Doctoral thesis*, Institute of Advanced Energy, Kyoto University, 2002.
- 19) H. Araki, T. Noda, W. Yang and A. Kohyama: *J. Nucl. Mater.* **307–311** (2002) 1210–1214.
- 20) A. J. Eckel and R. C. Bradt: *J. Am. Ceram. Soc.* **72** (1989) 455–458.
- 21) S. Bertrand, P. Forio, R. Pailler and J. Lamon: *J. Am. Ceram. Soc.* **82** (1999) 2465–2473.
- 22) W. Yang, A. Kohyama, Y. Katoh, H. Araki, J. Yu and T. Noda: *J. Am. Ceram. Soc.* **86** (2003) 851–856.